1068

Innate and Adaptive Immune Responses and Antitumor Activity Associated With ARV-6723, a PROTAC HPK1 Degrader, in Exhausted/Post-ICI Preclinical Settings

Anna C Van Acker, William Corwin, Wendy Wu, Albert DeBerardinis, Christopher Kuhlberg, Morena Scopel, Rebecca Conrad, Gregory Cadelina, Kim Davenport, Jennifer Pizzano, Angela Cacace, Eric Masson, John Corradi, Ignacio J Juncadella, Sean Landrette, XiaoZhe (Janet) Wang

Arvinas Operations, Inc., New Haven, CT, USA

Background

- HPK1, encoded by *MAP4K1*, is a serine/threonine protein kinase expressed predominantly in hematopoietic cells[1,2]
- HPK1 is a negative regulator of T-cell receptor signaling, reducing T-cell activation and proliferation and contributing to T-cell dysfunction and exhaustion[3,4]
- HPK1 also negatively regulates other immune-cell populations, including B cells, NK cells, and dendritic cells, through kinase-dependent and kinase-independent scaffolding functions[5–9]
- Although immunotherapies have improved outcomes across multiple solid-tumor types, many patients experience limited or transient benefit, with resistance commonly associated with T-cell dysfunction and exhaustion and an immunosuppressive TME[10,11]
- Novel immunotherapy approaches that modulate multiple aspects of antitumor immunity are needed to overcome resistance to ICIs and improve patient outcomes
- ARV-6723, a potent, selective, oral PROTAC HPK1 degrader, is being investigated as a potential immunotherapy in patients with advanced solid tumors and prior exposure to ICIs (NCT07749586; see poster 551)
- In vitro, ARV-6723 induced deep, sustained HPK1 degradation and durable pathway engagement, as well as increased T-cell IL-2 and NK-cell IFN-γ production, indicating restoration of function in exhausted T cells[12]
- Across multiple syngeneic mouse models spanning different TMEs, including ICI-resistant models, ARV-6723 monotherapy demonstrated potent antitumor activity that exceeded what was observed with ICIs or HPK1 inhibitors[12–14]
- ARV-6723 antitumor activity was associated with TME modulation, including increases in proinflammatory and decreases in anti-inflammatory immune-cell populations and peripheral cytokines[12–14]

Scan to view previously presented ARV-6723 preclinical data[12–14]

SITC Annual Meeting 2025

AACR IO Conference 2026

AACR Annual Meeting 2026

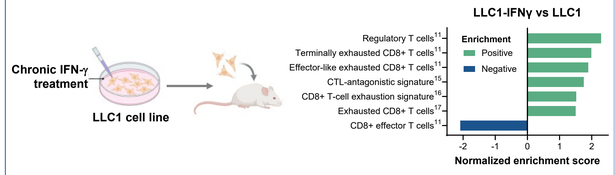
Objectives

- Evaluate ARV-6723 antitumor activity in post-ICI and ICI-resistant settings using human- and mouse-derived preclinical models
- Characterize ARV-6723 mechanism of action in post-ICI and ICI-resistant models by RNA expression analysis and multiplex immunofluorescence

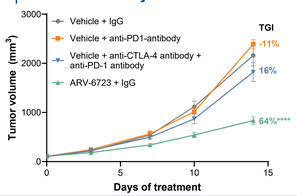
Society for Immunotherapy of Cancer (SITC) 2026 Annual Meeting
Phoenix, AZ, USA; November 4–8, 2026

In the LLC1-IFNγ mouse model of ICI resistance, ARV-6723 treatment demonstrated significant TGI, induced gene expression changes consistent with reduced T-cell exhaustion, and increased productive antitumor IFN activity, whereas ICIs had minimal effects

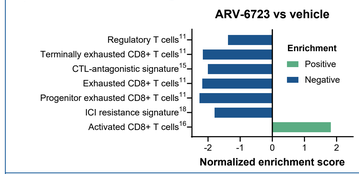
A | ICI-resistant LLC1-IFNγ model with a T-cell exhaustion phenotype



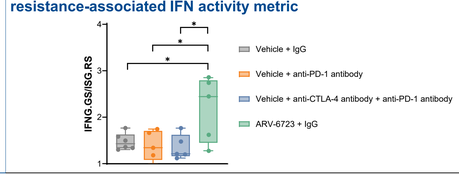
B | Antitumor activity



C | T-cell exhaustion signatures



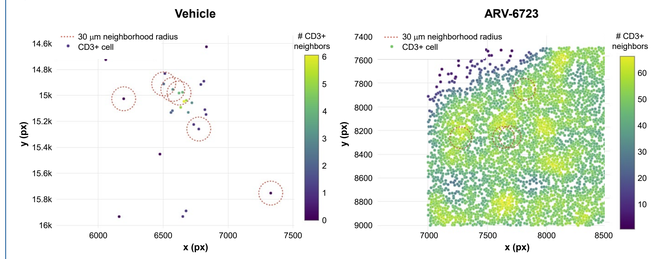
D | IFNG.GS/ISG.RS ratio: productive antitumor vs chronic resistance-associated IFN activity metric



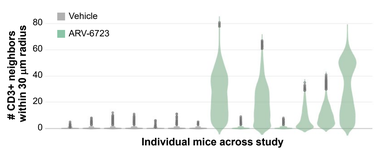
(**A**) Schematic detailing the generation of the LLC1-IFNγ mouse model through chronic in vitro treatment of the LLC1 cell line with IFN-γ and gene set enrichment analysis of RNA-seq data comparing LLC1-IFNγ tumors with parental LLC1 tumors; the profile was consistent with a previous report of this model.[11] (**B**) Tumor growth curves in C57BL/6 mice bearing subcutaneous LLC1-IFNγ tumors and treated with vehicle + IgG, ARV-6723 (30 mg/kg PO QD) + IgG, vehicle + anti-PD-1 antibody (10 mg/kg IP BIW), or vehicle + anti-CTLA-4 antibody (10 mg/kg IP BIW) + anti-PD-1 antibody (10 mg/kg IP BIW) for 14 days (n=8–10 per group). Percentage values represent mean percent change from vehicle. *P* values were calculated using one-way ANOVA with Dunnett's multiple-comparisons test vs vehicle. ****$P<0.0001$. (**C**) Gene set enrichment analysis of RNA-seq data from tumors harvested at the endpoint of the efficacy study shown in panel B comparing ARV-6723–treated with vehicle-treated tumors. (**D**) Bulk RNA-seq and gene set enrichment analyses were performed to compare ARV-6723– and vehicle-treated tumors, with additional pathway analysis assessing the IFNG.GS/ISG.RS ratio.[18] Quartile analysis was used to exclude outliers. Gene set scores were calculated using ssGSEA. The IFNG.GS/ISG.RS ratio was compared across groups using one-way ANOVA followed by Tukey's HSD test to adjust for multiple pairwise comparisons. *$P<0.05$.

In the LLC1-IFNγ model, ARV-6723 increased T-cell infiltration and proximity and cytotoxic T-cell density

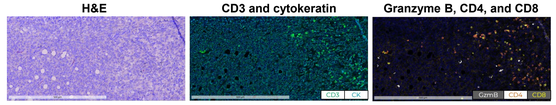
A | T-cell spatial distribution and neighboring cell analysis



B | Distribution of CD3⁺ neighbor counts per cell

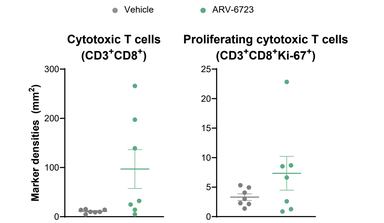


C | Intratumoral cytotoxic T cells



Representative images of tumors from mice treated with ARV-6723

D | Cytotoxic T-cell density



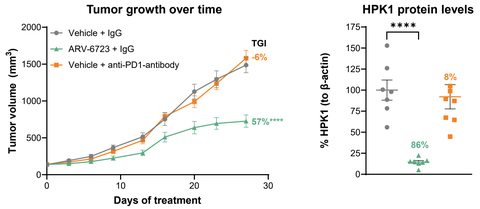
Neighboring-cell analysis was performed on multiplex immunofluorescence-stained FFPE sections of LLC1-IFNγ tumors harvested at the terminal endpoint of the efficacy study shown in upper left figure panel B. (**A**) Representative T-cell neighborhood maps of vehicle- and ARV-6723–treated tumors. (**B**) Quantification of the number of neighboring CD3⁺ T cells per index T cell across the entire tumor tissue. (**C**) Representative image of an ARV-6723–treated tumor stained for H&E, CD3, cytokeratin (tumor marker), granzyme B, CD4, and CD8. (**D**) Quantification of multiplex immunofluorescence staining to assess the density of CD3⁺CD8⁺ and CD3⁺CD8⁺Ki-67⁺ cells within tumor segments from vehicle- and ARV-6723–treated mice (n=7 per group).

In a humanized PDX model of acquired ICI resistance, ARV-6723 treatment demonstrated antitumor activity whereas an anti-PD-1 antibody did not, with increased T-cell infiltration, productive antitumor IFN activity, and immune-cell activation

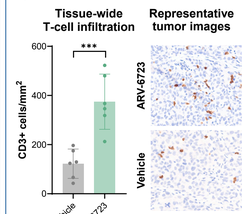
A | Antitumor activity and HPK1 degradation

Patient treatment history:

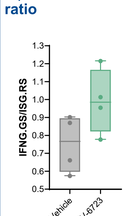
- Received nivolumab + relatlimab for 12 months
- Responded and then experienced disease progression
- Biopsy collected at time of disease progression



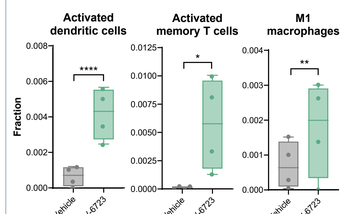
B | T-cell infiltration



C | IFNG.GS/ISG.RS ratio



D | Inferred immune-cell populations



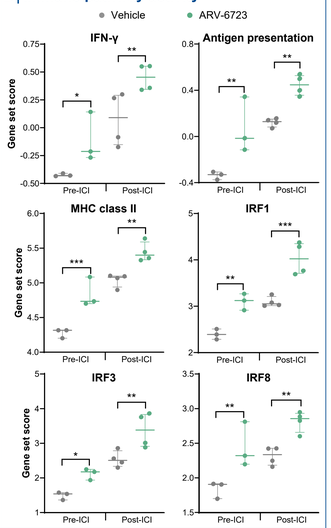
(**A**) Tumor growth curves in CD34⁺ humanized mice bearing subcutaneous CTG-4243 PDX tumors and treated with vehicle + IgG, ARV-6723 (30 mg/kg PO QD) + IgG, or vehicle + anti-PD-1 antibody (clinical-grade pembrolizumab, 5 mg/kg IP BIW) for 27 days (n=7–8 per group). Tumor HPK1 levels were assessed by western blotting at the study endpoint. (**B**) T-cell infiltration was assessed in IHC-stained FFPE tumor sections harvested at the terminal endpoint (n=6 per group). Staining was quantified by a board-certified pathologist. Representative images are shown at 400× magnification. (**C–D**) RNA-seq analyses of tumors harvested at the endpoint of the efficacy study shown in panel A, including gene set enrichment, immune-cell deconvolution, and assessment of the IFNG.GS/ISG.RS ratio. Quartile analysis was used to exclude outliers. The IFNG.GS/ISG.RS ssGSEA ratio was compared between groups using the Student's t-test. Immune cell fractions were inferred by iSort™ (CiberMed) and compared between groups using beta regression with Wald z tests, and *P* values were adjusted for multiple comparisons using Tukey's method. *$P<0.05$; **$P<0.01$; ***$P<0.001$; ****$P<0.0001$; $P=0.09$ for IFNG.GS/ISG.RS ratio (**C**).

Ex vivo ARV-6723 treatment increased IFN-γ signaling and antigen-presentation pathway activity and enhanced proinflammatory cytokine secretion following T-cell stimulation in both pre- and post-ICI PBMC samples

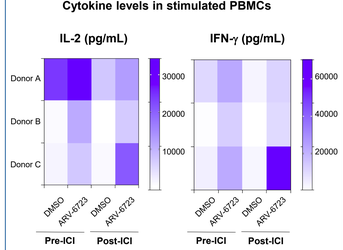
A | Patient-matched PBMC samples

Donor	A	B	C
Primary diagnosis	HNSCC	Gastric cancer	NSCLC
ICI treatment	Nivolumab	Nivolumab	Nivolumab
Treatment duration before sample collection	2–3 months	Unknown	Unknown

B | Immune pathway activity



C | Proinflammatory cytokine secretion



(**A**) Summary of patient-matched PBMC samples collected before and after initiation of ICI treatment. (**B**) RNA-seq and pathway analyses of PBMCs from donor A following 24 h ex vivo treatment with vehicle (DMSO) or ARV-6723 (100 nM; n=3 technical replicates per condition). (**C**) Cytokine analysis of supernatants from donors A–C following 24 h ex vivo treatment with vehicle (DMSO) or ARV-6723 (100 nM) and 6 h of CD3/CD28 stimulation. Cytokine levels were measured using the V-PLEX Proinflammatory Panel 1 Human Kit. Gene set scores were compared between groups using limma. *$P<0.05$; **$P<0.01$; ***$P<0.001$.

Conclusions

- Single-agent ARV-6723 demonstrated greater antitumor activity than standard-of-care ICIs in mouse models representing clinically relevant mechanisms of ICI resistance
- Mechanistic analyses demonstrated ARV-6723–mediated remodeling of innate and adaptive immune compartments toward an antitumor phenotype in human- and mouse-derived models, including settings of T-cell exhaustion and prior ICI treatment
- These preclinical data support investigation of ARV-6723 in patients with advanced solid tumors following ICI treatment, a population with high unmet medical need

References

1. Hu MC, et al. Genes Dev. 1996;10:2251-64.
2. Sawasdikosol S, Burakoff S. eLife 2020;9:e55122.
3. Liou J, et al. Immunity. 2000;12(4):399-408.
4. Ling P, et al. J Biol Chem. 2001;276(22):18908-14.
5. Alzabin S, et al. J Immunol. 2009;182(10):6187-94.
6. Liu J, et al. PLoS ONE. 2019;14(3):e0212670.
7. You D, et al. J Immunother Cancer. 2021;9(1):e001402.
8. Bader A, et al. Eur J Immunol. 2022;52(5):760-769.
9. Choi WS, et al. Adv Sci. 2024;11(29):e2400920.
10. Seto T, et al. Med Sci. 2019;7(2):14.
11. Memon D, et al. Cancer Cell. 2024;42(2):209-224.e9.
12. Corwin W, et al. Society for Immunotherapy of Cancer Annual Meeting 2025;1158.
13. Van Acker A, et al. AACR Immuno-Oncology Conference 2026;C041.
14. Van Acker A, et al. AACR Annual Meeting 2026;4309.
15. Jiang P, et al. Nat Med. 2018;24:1550-1558.
16. Giordano M, et al. EMBO J. 2015;34:2042-58.
17. Bengsch B, et al. Immunity. 2018;48:1029-1045.
18. Benci JL, et al. Cell. 2019;178:933-948.

Abbreviations

ANOVA=analysis of variance; BIW=twice weekly; CK=cytokeratin; CTL=cytotoxic T-lymphocyte; CTLA-4=cytotoxic T-lymphocyte–associated protein 4; DMSO=dimethyl sulfoxide; FFPE=formalin-fixed, paraffin-embedded; GzmB=granzyme B; H&E=hematoxylin and eosin; HNSCC=head and neck squamous cell carcinoma; HPK1=hematopoietic progenitor kinase 1; HSD=honestly significant difference; ICI=immune checkpoint inhibitor; IFN=interferon; IFNG.GS=interferon gamma gene signature; IgG=immunoglobulin G; IHC=immunohistochemistry; IL=interleukin; IP=intraperitoneal; IRF=interferon regulatory factor; ISG.RS=interferon-stimulated gene resistance signature; MHC=major histocompatibility complex; NK=natural killer; NSCLC=non-small cell lung cancer; PBMC=peripheral blood mononuclear cell; PD-1=programmed cell death protein 1; PDX=patient-derived xenograft; PO=orally; PROTAC=PROteolysis TArgeting Chimera; QD=once daily; RNA-seq=RNA sequencing; ssGSEA=single-sample gene set enrichment analysis; TGI=tumor growth inhibition; TME=tumor microenvironment

Contact
Anna Van Acker:
anna.chiarella@arvinas.com

Scan to view a copy of this poster

Acknowledgments
This research was funded by Arvinas, Inc. Medical writing support was provided by Joanna Bloom of Arvinas Operations, Inc.